NENE 2013
September 9-12
BLED-SLOVENIA
22nd International Conference Nuclear Energy for New Europe

Modelling of a Passive Catalytic Recombiner for Hydrogen Mitigation by CFD Methods

Antoni Rożeń
Warsaw University of Technology, Faculty of Chemical and Process Engineering
Waryńskiego 1, 00-645 Warszawa, Poland
a.rozen@ichip.pw.edu.pl

ABSTRACT

Four turbulence models (k-ω, k-ε, intermittency, RSM) have been applied in CFD simulations of: gas flow, heat and mass transport, and chemical surface reactions occurring in a passive catalytic recombiner used to remove hydrogen from safety containments of light water nuclear reactors. It was found that differences in model predictions increase with increasing gas flow rate, while at low gas flow rates simulation results converge to those obtained for a limiting case of laminar flow. Heat and mass transfer taking place in the gas phase were identified as essentially two dimensional processes unlike heat exchange with the environment. Large Eddy Simulation technique was used to select the turbulence model giving the best prediction of the hydrogen recombination rate.

1 INTRODUCTION

Hydrogen, generated during normal operation of a light water nuclear reactor and in emergency situations such as overheating of a reactor core, accumulates in a cooling system and in a reactor safety containment. This can lead to a local increase of the hydrogen concentration above its flammability limit and hydrogen ignition, and a possible flame propagation in the reactor safety containment [1]. Different methods are used in practice to mitigate risk of uncontrolled hydrogen ignition, e.g.: controlled hydrogen ignition, catalytic recombination, dilution of hydrogen due to mixing, injection of neutral gas, venting of the safety containment [1]. Catalytic recombination of hydrogen with oxygen is conducted in passive autocatalytic recombiners (PAR) consisting of a system of plates or beds covered by platinum or palladium catalysts [2]. Hydrogen and oxygen are adsorbed on the catalyst surface, react spontaneously producing water, which is desorbed to the gas phase. The reaction heat produces natural convection flow through PAR, exhausting humid, hydrogen depleted gas and drawing fresh hydrogen rich gas from below. PAR activates itself when the hydrogen concentration exceeds 1-2% v/v in air and requires neither external power nor supervision.

Performance of different PAR designs were studied not only experimentally but also by means of CFD methods e.g. [2,3,4]. In most cases CFD studies were conducted with no proper modelling of the heat transfer between PAR external walls and the surrounding air. The gas flow inside PAR is modelled either as the fully laminar flow or as the turbulent one. Hence, the main aim of this work was to test different turbulence closure hypotheses in modelling of the gas flow, the heat and mass transport and the surface reactions proceeding in PAR and compare results with those obtained for the limiting case of the fully laminar flow as well as with results obtained by means of Large Eddy Simulations technique (LES). The second aim was to propose a method to determine the real heat transfer rate from PAR external walls to the environment.

2 MODELLING DETAILS

CFD simulations were conducted for PAR geometry from REKO-3 test facility [5]. This recombiner is a box type device consisting of three sections: inlet, recombiner and outlet as shown in Figure 1. The central recombiner section comprises a set of four stainless steel plates covered with platinum catalyst. The catalyst plates divide the central zone into five vertical rectangular channels. A CFD software package Ansys Fluent 14.5 was used to model gas flow, other transport processes and chemical reactions occurring in PAR. The numerical simulations were conducted in 2D as well as in 3D geometry of the recombiner. It was assumed that a hydrogen-air-steam mixture behaves inside PAR like an ideal gas, hence its density was determined from the ideal gas law. The kinetic theory of gas was applied to calculate such gas properties as: thermal conductivity (λ, W/(m·K)), dynamic viscosity (μ, Pa·s), coefficients of molecular and thermal diffusivity of gas components (D_i and D_{Ti}, m^2/s). The specific heats of gas components (c_{Pi}, J/(kg·K)) were calculated from polynomial correlations implemented in Ansys Fluent, while the specific heat of the gas mixture was determined as the mass average of the specific heats of all gas components. The inlet gas contained 4% v/v of hydrogen and 96% v/v of dry air and its temperature was equal 298 K; at these conditions density and viscosity of gas are equal to ρ=1,17 kg/m3 and $\mu=1{,}85\cdot10^{-5}$ Pa·s. According to Reinecke et. al [5] the catalyst plates and PAR housing were made from stainless steel. Hence, typical values of density, specific heat and thermal conductivity of stainless steel were used in simulations of heat conduction in the construction parts of PAR: ρ_S=7700 kg/m^3, c_{PS}=460 J/(kg·K), λ_S=25 W/(m·K).

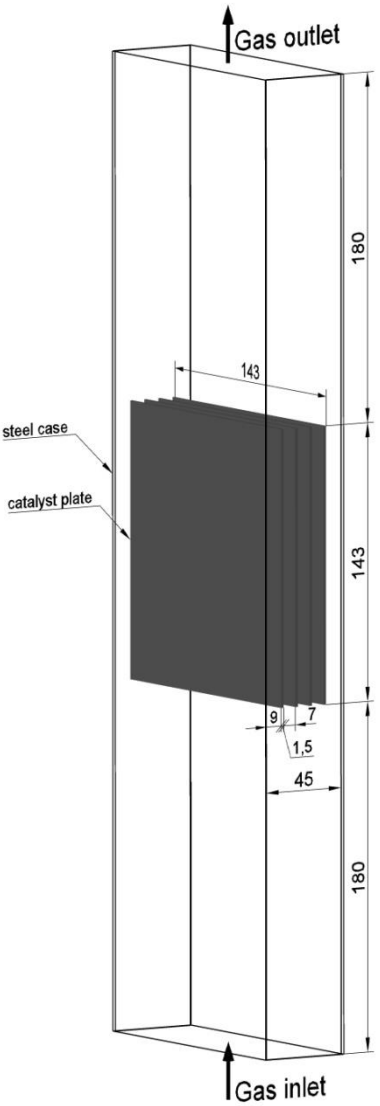

Figure 1. Geometry of PAR.

The heat generated in the recombination reactions is mainly absorbed by the gas phase but some part of it can be transferred to the environment through PAR walls by natural convection and thermal radiation. The natural heat convection rate is given by equation

$$Q_\alpha = \alpha A_w (T_w - T_f) \tag{1}$$

where A_w is the wall area, T_w is the wall temperature and T_f=298 K is the environment temperature. The convective heat coefficient α (W/(K·m^2)) was estimated from McAdams correlation for vertical flat walls [6]

$$Nu = 0{,}59 Gr^{0.25} Pr^{0.25}, \quad Gr \cdot Pr < 10^9 \tag{2}$$

Nusselt, Grashof and Prandtl numbers appearing in eq. (2) are defined as follows

$$Nu = \frac{\alpha L}{\lambda}, \quad Gr = \frac{g\beta(\bar{T}_w - T_f)L^3\rho^2}{\mu^2}, \quad Pr = \frac{c_P \mu}{\lambda} \tag{3}$$

where L is the wall height, β (1/K) is the thermal expansion coefficient of air and $\bar{T}_w$ is the average wall temperature. Air parameters in eq.(3) were calculated at the mean temperature

$$\bar{T} = 0.5(\bar{T}_w + T_f) \tag{4}$$

The heat radiation rate between the catalyst plates, walls and environment, can be found from Stefan-Boltzman equation [6]

$$Q_r = \varepsilon A C_0 (T_2^4 - T_1^4), \quad C_0 = 5.669 \cdot 10^{-8}\, W/(m^2 K^4) \tag{5}$$

where ε and A are apparent emissivity and radiant surface area, while T_1 and T_2 are the temperatures of the radiant surfaces. The characteristic emissivities of PAR construction elements were as follows: the catalyst covered surfaces 0.95, PAR walls 0.25, the environment 1. Ansys Fluent "surface to surface" algorithm was used to determine values of the emissivity ε and the surface area A from the geometric configuration of the radiant surfaces. Due to the fact that the average temperatures of PAR external surfaces were not known a priori their values had to be updated during CFD simulations in order to calculate the convective heat coefficient for these surfaces.

The hydrogen recombination reaction proceeds according to an over-all scheme

$$H_2 + \frac{1}{2} O_2 \rightarrow H_2O \tag{6}$$

and generates $2.483 \cdot 10^5$ kJ of heat per kmol of hydrogen. It was assumed that hydrogen reacts with oxygen only at the catalyst plates without any combustion in the gas phase. Even then, according to Fridel et. al [7] seven reaction steps should be considered during modelling of the recombination kinetics. However for low hydrogen concentrations in the gas phase (less than 5% v/v) and for low humid air conditions the complicated kinetic model can be reduced to a single kinetic equation in the catalyst ignition regime [8]

$$r_{H_2} = 4.695 \sqrt{T}\, c_{H_2}^2 c_{O_2}^{-1}, \quad \text{kmol/(s} \cdot \text{m}^2\text{)} \tag{7}$$

where c_i denotes molar concentration of the reactants in the gas phase.

The above physical and kinetic data were incorporated into a system consisting of: a continuity and momentum equations, enthalpy balance equations of gas and steel, and material balance equations for the gas components and following boundary conditions:

- constant inlet gas velocity v_{in} (=0.2÷1.6 m/s), gas temperature T_{in}(=298 K), and gas composition $x_{in,i}$ ($x_{in,H2}$=0.04, $x_{in,O2}$=0.201, $x_{in,N2}$=0.759, $x_{in,H2O}$=0)
- equal mass flow rates at the inlet and the outlet of PAR,
- zero gas velocity at the catalyst plates and at PAR walls,
- zero mass flux at PAR walls,
- heat flux at the external PAR walls given by eqs (1) and (5).

PAR operating pressure was set to the atmospheric pressure and the gravitational acceleration was activated in the Fluent solver module to account for buoyancy effects.

Simulations were conducted for laminar and turbulent flow conditions. In the second case four different Reynolds average stress models (RANS) were applied:
a) k-ω model (2 eqs),
b) k-ε model (2 eqs),
c) transition shear stress model (intermittency model, 4 eqs),
d) Reynolds stress model (RSM, 5 eqs in 2D and 7 eqs in 3D).
Additionally Large Eddy Simulation method (LES) with Smagorinski-Lilly sub-grid turbulence model was used to calculate the velocity, temperature and concentration fields inside PAR for the highest inlet velocity v_{in}=1.6 m/s.

3 RESULTS AND DISSCUSION

The gas flow in inside the recombiner can by characterized by Reynolds number

$$Re = \frac{\bar{v} d_h \rho}{\mu} \tag{8}$$

where $\bar{v}$ denotes the average gas velocity and d_h is the hydraulic diameter. When the inlet gas velocity equals 1.6 m/s Reynolds number is close to 7100 at the inlet, then it drops below 1000 in the central PAR section, while in the outlet zone Reynolds number increases to 5000. Reducing the inlet velocity decreases proportionally all these Reynolds numbers. On the other hand, Grashof number characterizing natural gas convection in the central section of PAR is of the order of 10^7. Hence, even if a developed turbulent flow existed in the inlet section of PAR turbulence would quickly decay in the narrow and long channels between the catalyst plates. Indeed, CFD modelling confirmed turbulence dumping in the central section of PAR. Figure 2 clearly shows how the ratio of turbulent to molecular gas viscosity (μ_t/μ) decreases below unity when gas flows into the narrow channels for all RANS models. Turbulence is restored when gas leaves these channels. RSM and k-ε model predicted the fastest growth of the turbulent viscosity in the upper PAR section. This is typical for these models usually recommended to simulations of turbulent flows characterized by high Reynolds numbers. On the contrary, k-ω and intermittency models, which are designed for low Reynolds number turbulent flows, predicted high values of the viscosity ratio (μ_t/μ) in the channels entrance sections and the slow growth of the viscosity ratio (especially k-ω model) above the catalyst plates. In fact differences between the particulate model predictions were so large that logarithmic grading of the colour scale had to be used in Fig. 2.

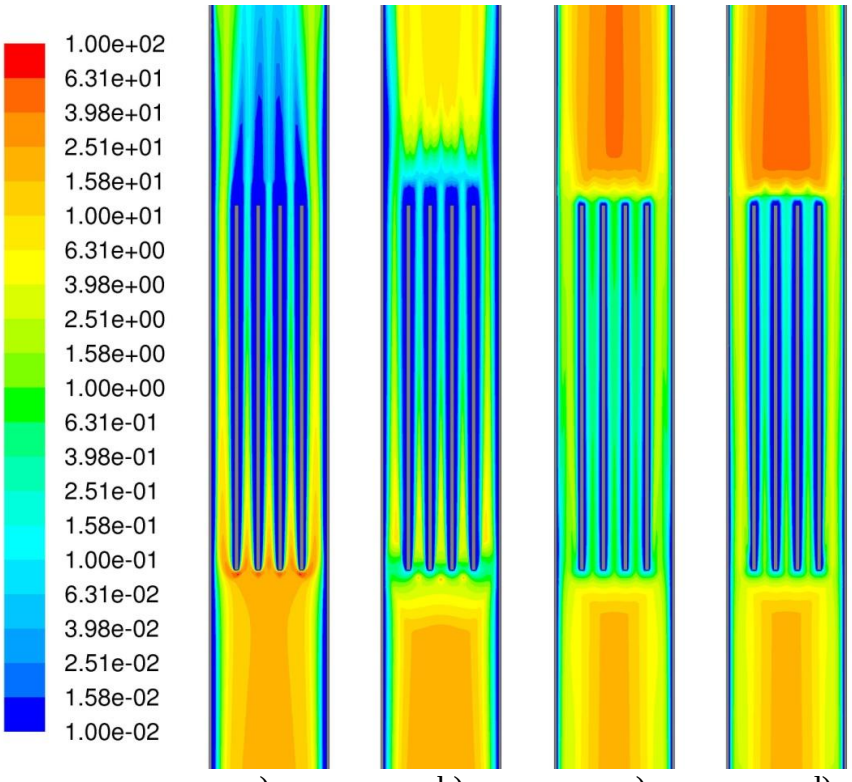

Figure 2. Ratio of turbulent to molecular gas viscosity; v_{in}=1.6 m/s, 2D PAR geometry; a) k-ω model, b) intermittency model, c) RSM model, d) k-ε model.

Far less but still noticeable differences characterize the hydrogen distribution inside PAR as shown in Figure 3. The fastest reduction of the hydrogen concentration and the largest differences in CFD results can be observed inside the entrance section of the channels between the catalyst plates, where the reactant concentration gradients are maximal and the rate of the reactants transport towards the catalyst surface is the highest. The reactant concentration gradients decrease further along the channels and so the recombination rate, which becomes controlled by the rate of reactants transport to the catalyst surface. The quickest hydrogen depletion rate was predicted by k-ω model because the turbulent viscosity and so the turbulent diffusivities of the reactants were higher in the channels entrance section than those calculated by means of other turbulence models. An exact examination of Fig. 3 reveals also that the hydrogen concentration exceeded its inlet value (4 % v/v) in the vicinity of PAR walls and at the leading edges of the catalyst plates (not covered by the catalyst). It was caused by thermal diffusion of hydrogen, which in the regions of the highest temperature gradients in the gas phase became eventually faster than molecular diffusion.

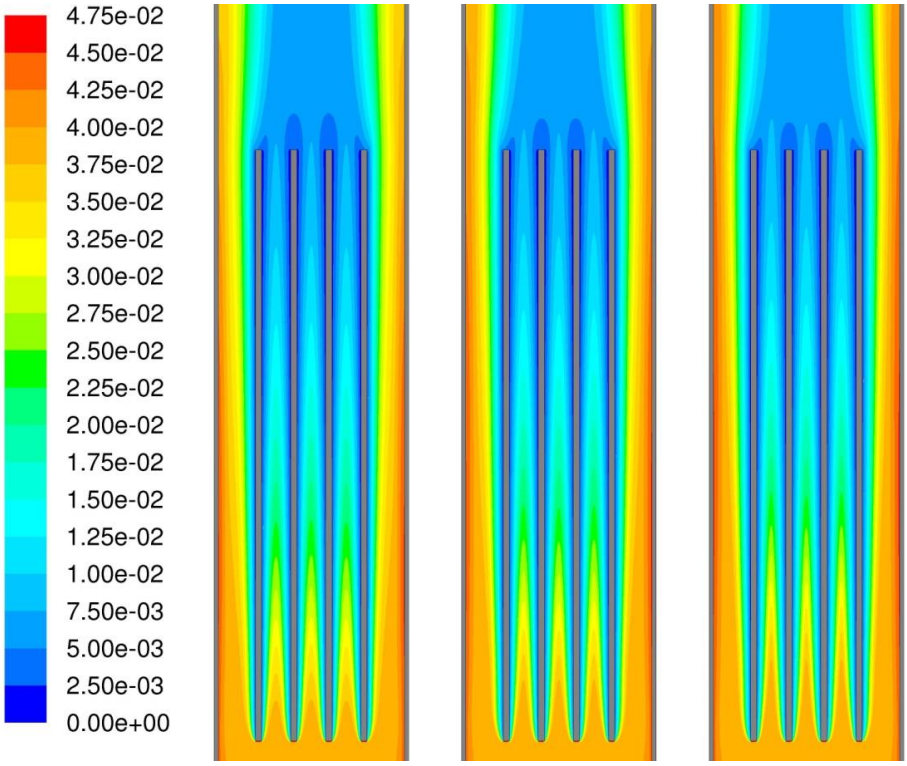

Figure 3. Molar fraction of hydrogen in the gas mixture; v_{in}=1.6 m/s, 2D PAR geometry: a) k-ω model, b) intermittency model, c) laminar flow.

The flow laminarization in the central section of PAR is almost complete when the gas inlet velocity is reduced below 0.4 m/s. Hence, there is no surprise that the final hydrogen conversion degree, predicted by RANS models, approached its limiting value obtained for laminar flow conditions (v_{in} < 0.4 m/s), as illustrated in Figure 4. At the higher inlet velocities the hydrogen conversion degree obtained by the intermittency model was closest to that determined for laminar flow, while k-ω model predicted the highest conversion degree.

The results of CFD simulations in the two-dimensional PAR geometry have been presented so far. Their comparison with results of CFD simulations conducted for the three-dimensional PAR geometry is given in tables 1 and 2. It can be seen that the overall recombination rates obtained in 2D and 3D cases are close to each other. This indicates that the simulated species transport inside the central section of PAR is virtually two-dimensional.

Indeed contours of the hydrogen molar fraction plotted at five different horizontal cross-sections of PAR in Figure 5 broadly confirm this supposition. The lowest cross-section in Fig. 5 was positioned just below the leading edges of catalyst plates, the second one at the half height of these plates, the third one just above the trailing edges of the catalyst plates, while the fourth and the fifth ones in the upper section of PAR.

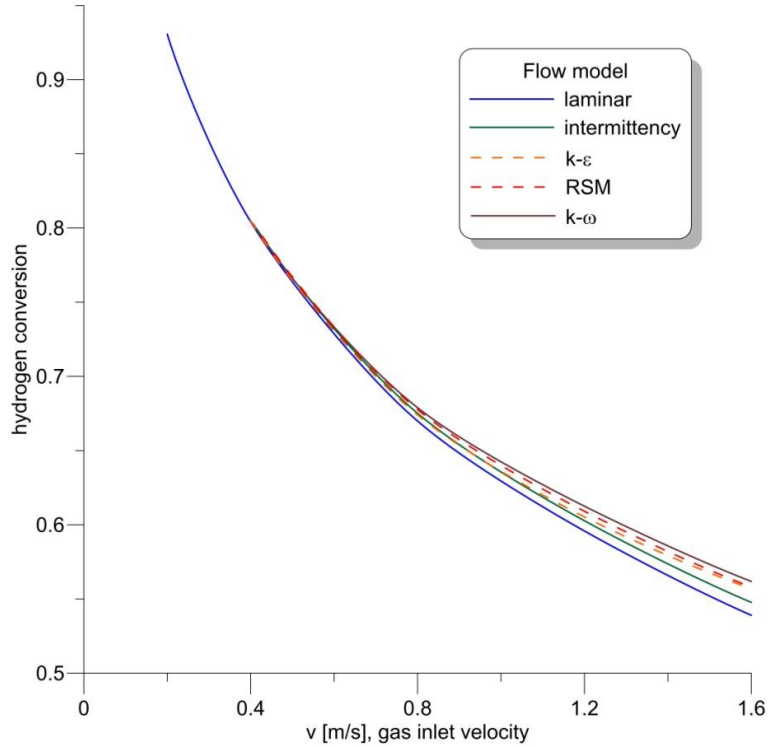

Figure 4. Effect of the gas inlet velocity on the final hydrogen conversion; 2D PAR geometry.

Table 1: Results of CFD modelling; gas inlet velocity 1.2 m/s

Flow model	2D geometry		3D geometry	
	$\Delta\dot{m}_{H_2}$ [kg/h]	Q_W/Q_S	$\Delta\dot{m}_{H_2}$ [kg/h]	Q_W/Q_S
Laminar	0.0546	0.0742	0.0549	0.1390
k-ω	0.0562	0.0721	0.0560	0.1369
Intermittency	0.0552	0.0723	0.0554	0.1365
RSM	0.0558	0.0679	0.0562	0.1298
k-ε	0.0555	0.0699	0.0558	0.1326

Table 2: Results of CFD modelling; gas inlet velocity 1.6 m/s

Flow model	2D geometry		3D geometry	
	$\Delta\dot{m}_{H_2}$ [kg/h]	Q_W/Q_S	$\Delta\dot{m}_{H_2}$ [kg/h]	Q_W/Q_S
laminar	0.0659	0.0672	0.0660	0.1252
k-ω	0.0687	0.0625	0.0682	0.1203
intermittency	0.0670	0.0647	0.0669	0.1217
RSM	0.0682	0.0568	0.0684	0.1106
k-ε	0.0681	0.0582	0.0682	0.1128
LES	–	–	0.0669	0.1202

The concentration contours presented in Figure 5 were obtained by two models: the intermittency model and LES model. The second approach is based on the observation that kinetic turbulent energy and flow anisotropy apply mainly to large scale fluid motions,

depending on the actual system geometry, while the final dissipation of kinetic energy and flow isotropy are observed at smaller scales. LES model directly resolves the large turbulent eddies while the sub-grid turbulent eddies are subject to an averaging procedure, e.g. a sub-grid Smagorinski-Lilly model. LES model can be used in a wider range of Reynolds number than RANS models and it is well suited to simulation of low Reynolds anisotropic flows characteristic for PAR. In the considered case a comparison of the instantaneous and the averaged concentration distributions revealed that the large eddies affected the hydrogen distribution in the side channels of the central and in the entire outlet PAR section, while the concentration field in the inner channels was practically undisturbed – Fig. 5. The intermittency model was chosen for comparison in Fig. 5 because it predicted almost the same recombination rate as LES model – table 2. This result should be confirmed experimentally before any further conclusions can be drawn. Similarly as in 2D case the recombination rates given by the intermittency model were closest to those determined for laminar flow in 3D case, while the k-ω, k-ε and RSM models predicted higher recombination rates.

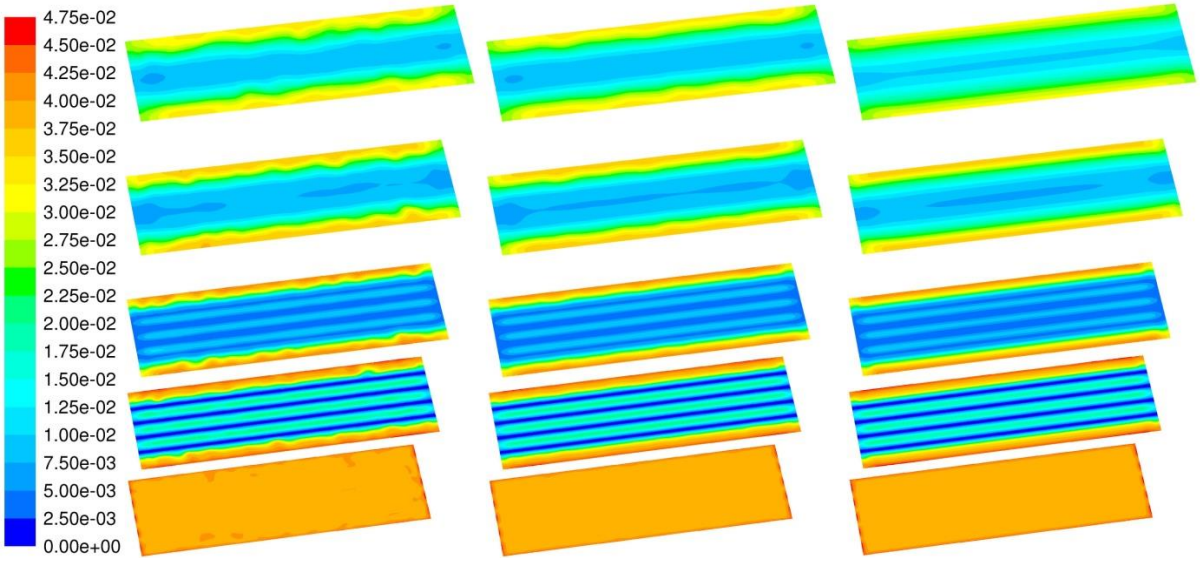

Figure 5. Molar fraction of hydrogen in the gas mixture; v_{in}=1.6 m/s, 3D PAR geometry:
a) LES – instantaneous contours, b) LES – time averaged contours, c) intermittency model.

The heat generated during the hydrogen recombination is transferred from the catalyst plates by: convection to the gas phase, conduction and radiation to PAR steel case. When the recombiner walls are not insulated heat can escape to the surrounding by natural convection and radiation. The results of CFD simulations indicate that the heat transferred to PAR walls raised their temperature in the central PAR section above gas temperature inside the recombiner. The calculated ratio of the heat transferred by PAR walls to the total heat of the hydrogen recombination (Q_W/Q_S) is presented in tables 1 and 2. The heat transfer rate to the surrounding is approximately twice smaller for 2D than for 3D PAR geometry. This is so because the temperature of the narrower side walls supporting the very hot catalyst plates is considerably higher than temperature of the wider front and back walls as shown in Figure 6.

The results of CFD simulations of the hydrogen recombination in PAR allow to conclude that a key issue in a correct prediction of the overall recombination rate is a resolution of the gas flow and other transport processes in the central section of the device where the flow laminarization occurs. The comparison of the hydrogen recombination rates predicted by four RANS models and LES model showed that each turbulence model gave different results. Only the intermittency and LES models predicted the same recombination rates. However an experimental verification (e.g. comparison of measured and calculated

turbulence intensity) is necessary to determine the best closure hypothesis. It also turned out that mass transport processes occurring in the central PAR section are two-dimensional unlike heating of PAR housing, which influences the rate of heat escape to the environment and may cause dangerous build-up of the hydrogen concentration in the gas adjacent to PAR walls.

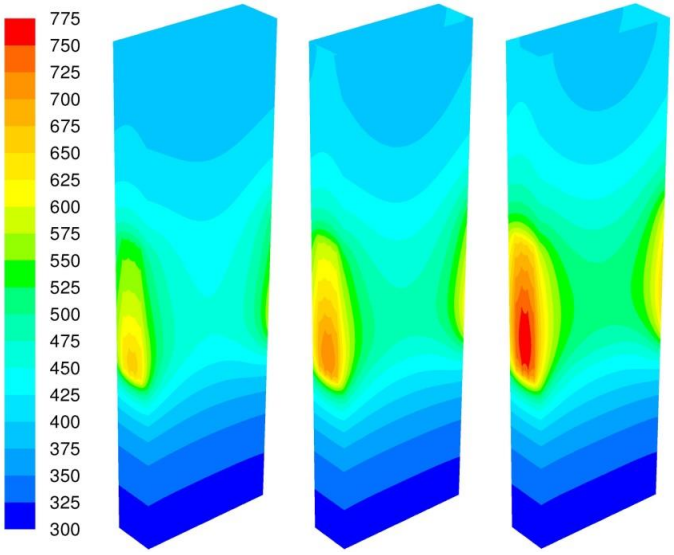

Figure 6. Temperature of PAR external walls: a) v_{in}=0.4 m/s, b) v_{in}=0.8 m/s, c) v_{in}=1.6 m/s.

Acknowledgments. This work was financially supported by The National Centre of Research and Development in Poland (grant no. SP/J/7/170071/12).

REFERENCES

[1] IAEA-TECDOC-1661, "Mitigation of Hydrogen Hazards in Severe Accidents in Nuclear Power Plants", IAEA, Vienna 2011.

[2] E.A. Reinecke, A. Bentaib, S. Kelm, W. Jahn, N. Meynet, C. Caroli, "Open issues in the applicability of recombiner experiments and modelling to reactor simulations", Prog. Nucl. Energ., 52, 2010, pp. 136-147.

[3] B. Gera, P.K. Sharma, R.K. Singh, "Numerical Study of Passive Catalytic Recombiner for Hydrogen Mitigation", CFD Letters, 2, 2010, pp. 123-136.

[4] D.M. Prabhudharwadkar, K.N. Iyer, Simulations of hydrogen mitigation in catalytic recombiner: Part-II: Formulation of a CFD model, Nucl. Eng. Des., 241, 2011, pp. 1758-1767.

[5] E.A. Reinecke, I.M. Tragsdorf, K. Gierling, "Studies of innovative hydrogen recombiners as safety devices in the containment of light water reactors", Nucl. Eng. Des., 230, 2004, pp. 49-59.

[6] C.O. Bennett, J.E. Myers, „Momentum, Heat and Mass Transfer", McGraw Hill Book Company, Inc., New York, 1962.

[7] E. Friedel, A. Rosen, B. Kasemo, "A laser induced fluorescence study on OH desorption from Pt in H_2O/O_2 and H_2O/H_2 mixtures", Langmuir, 10, 1994, pp. 699-708.

[8] D.M. Prabhudharwadkar , P.A. Aghalayam, K.N. Iyer, "Simulations of hydrogen mitigation in catalytic recombiner: Part-I: Surface chemistry modelling", Nucl. Eng. Des., 241, 2011, pp. 1746-1757.